BBA - Bioenergetics 1863 (2022) 148597

Contents lists available at ScienceDirect

BBA - Bioenergetics

journal homepage: www.elsevier.com/locate/bbabio

A biophysical basis for the emergence of the genetic code in protocells

Stuart A. Harrison, Raquel Nunes Palmeira, Aaron Halpern, Nick Lane *

Department of Genetics, Evolution and Environment, University College London, Darwin Building, Gower Street, London WC1E 6BT, United Kingdom of Great Britain and Northern Ireland

ARTICLE INFO

Keywords:
Origin of life
Genetic code
Protocells
Autotrophy

ABSTRACT

The origin of the genetic code is an abiding mystery in biology. Hints of a 'code within the codons' suggest biophysical interactions, but these patterns have resisted interpretation. Here, we present a new framework, grounded in the autotrophic growth of protocells from CO_2 and H_2. Recent work suggests that the universal core of metabolism recapitulates a thermodynamically favoured protometabolism right up to nucleotide synthesis. Considering the genetic code in relation to an extended protometabolism allows us to predict most codon assignments. We show that the first letter of the codon corresponds to the distance from CO_2 fixation, with amino acids encoded by the purines (G followed by A) being closest to CO_2 fixation. These associations suggest a purine-rich early metabolism with a restricted pool of amino acids. The second position of the anticodon corresponds to the hydrophobicity of the amino acid encoded. We combine multiple measures of hydrophobicity to show that this correlation holds strongly for early amino acids but is weaker for later species. Finally, we demonstrate that redundancy at the third position is not randomly distributed around the code: non-redundant amino acids can be assigned based on size, specifically length. We attribute this to additional stereochemical interactions at the anticodon. These rules imply an iterative expansion of the genetic code over time with codon assignments depending on both distance from CO_2 and biophysical interactions between nucleotide sequences and amino acids. In this way the earliest RNA polymers could produce non-random peptide sequences with selectable functions in autotrophic protocells.

1. Introduction

The genetic code offers tantalising clues to its own origins - a 'code within the codons' [1]. The first base in the triplet codon links the amino acid encoded with a shared precursor, implying a relationship between codons and biosynthetic pathways [1–3]. The second position of the anticodon is associated with the hydrophobicity of the amino acid encoded [4,5]. These associations have been identified both in biological systems with anticodon enrichments in aptamers [6,7] and through experimental methods [8–11]. Experimental identification of interactions however is difficult to definitively prove. The third position is agreed to have less coding information but has been linked to amino acid 'complexity' and molecular size before [1,12]. These patterns imply that direct biophysical interactions between amino acids and their cognate codons or anticodons fashioned at least some of the genetic code. Both the co-evolution and stereochemical hypotheses have complex histories in the literature, with proponents for and against the proposals [13–16]. The code within the codons remains deeply enigmatic.

The coevolution of metabolism and the code plainly depends on the actual structure of metabolism. Most hypotheses either assume heterotrophic origins or avoid specifying a particular autotrophic metabolism [1–3,17–19]. Di Giulio [18] has noted that a heterotrophic origin of amino acids is not easy to reconcile with the coevolution hypothesis, as it implies the earliest ten amino acids were simply taken from the environment. If so, then it is hard to see how their remote synthesis could correspond to coevolution patterns found in the code. But autotrophic origins are also difficult to reconcile with coevolution if the earliest catalysts of amino-acid biosynthesis were peptidated tRNAs, as normally assumed [18]. If that were the case, then where did the amino acids required for peptidation come from? One possible reconciliation is that simple dinucleotides bound the precursor of the amino acid coded and catalysed its transformation to the cognate amino acid [19]. While this ingenious notion has some theoretical (quantum mechanical) support [20] these ideas all tend to conflict with life as a guide to the origins of metabolism [21]. Neither the deeply conserved chemistry that underpins the mechanism of translation nor the universally conserved

* Corresponding author.
E-mail address: nick.lane@ucl.ac.uk (N. Lane).

https://doi.org/10.1016/j.bbabio.2022.148597
Received 12 April 2022; Received in revised form 27 June 2022; Accepted 13 July 2022
Available online 19 July 2022
0005-2728/© 2022 The Authors. Published by Elsevier B.V. This is an open access article under the CC BY license (http://creativecommons.org/licenses/by/4.0/).

pathways of amino-acid biosynthesis operate in this way. Instead, we favour a possible link with autotrophic protometabolism, which has gained strong experimental support in recent years.

Phylogenetics indicates that the last universal common ancestor (LUCA) was likely autotrophic and chemiosmotic, growing from H_2 and CO_2 via the acetyl CoA pathway and reverse incomplete Krebs cycle, the gateway into the universally conserved core of metabolism [22–29]. Recent experiments are confirming what has long been predicted by theoretical thermodynamics [30–33]: the chemistry of the universal core of metabolism can indeed occur spontaneously in the absence of genes and enzymes. Starting with CO_2 and H_2 (or reducing equivalents), intermediates in the acetyl CoA pathway and reverse Krebs cycle form spontaneously [34–36]. Non-enzymatic equivalents of glycolysis, the pentose phosphate pathway [37,38] and gluconeogenesis [39] have been identified as well. Multiple syntheses of amino acids from α-keto acids by direct reductive amination [40,41], and by transamination reactions [42] can also take place. Long-chain fatty acids can be formed by hydrothermal Fischer-Tropsch-type synthesis which chemically resembles the process of fatty acid elongation [43–45]. Recent work suggests that nucleobases might also be formed following the universally conserved biosynthetic pathways, using metal ions as catalysts [46].

The endergonic barrier to the first steps of CO_2 reduction can be lowered by proton gradients across Fe(*Ni*)S barriers [47], driving CO_2 fixation through vectorial electrochemistry in a similar way to cells [23,29,48–50]. Mathematical modelling shows that, in principle, dynamic proton gradients could drive the autotrophic growth of protocells in a 'monomer world' (i.e. lacking RNA and peptides; [24]) in which CO_2 fixation is catalysed by organically chelated FeS clusters associated with the membrane [51,52]. Experimental work confirms that protocells with mixed-amphiphile membranes are stable under the necessary conditions [53,54], and that cysteine at pH 9 acts as a ligand to form redox-active 4Fe4S clusters equivalent to those in ferredoxin [55]. Together, these findings suggest that the coupling of proton gradients to autotrophic protometabolism could drive protocell growth from H_2 and CO_2 in far-from-equilibrium environments such as alkaline hydrothermal vents [23,25,28,29,50]. The key point is that amino-acid biosynthesis would take place via a biomimetic protometabolism in autotrophically growing protocells.

Here we rationalise the possible emergence of the genetic code in the context of autotrophically growing protocells. Protometabolic reactions mimicking the core of extant metabolism and nucleotide polymerization are assumed to take place and can generate short sequences of RNA, which would initially have only possessed ribozymatic activity and lacked genetic information. Beginning with the universal core of autotrophy, we show a close relationship between the first position of the codon and the distance from CO_2 fixation; between purines at the second position and the hydrophobicity of amino acid; and between the properties of the codon and the length of the amino acids encoded. These simple rules allow us to assign the cognate amino acid to the large majority of codons, corroborating the idea that the code coevolved with autotrophic metabolism, with direct biophysical relationships between amino acids and random RNA strings.

2. The first codon position corresponds to distance from CO_2 fixation

The standard genetic code specifies 20 different amino acids which are universal across all domains of life. Yet abiotic syntheses of amino acids both in laboratory and environmental settings show substantially greater structural variation than in life, raising the question of why specific amino acids were incorporated into a genetic code. A protometabolic perspective on the genetic code neatly resolves this issue. By assuming that the chemistry that constitutes the conserved core of metabolism was the predominant prebiotic chemistry, the amino acid complement available is specified by this network. Further selection may depend on the self-reactivity of chemical species such as that proposed by Hendrickson, Wood and Rathnayake [56] discussed further in the SI.

The protometabolism hypothesis places a new emphasis on the importance of extant metabolism for understanding the emergence of the genetic code. Fig. 1 shows a metabolic map, beginning with CO_2 and proceeding to the 20 standard amino acids. Rather than reconstructing the pathway through phylogenetic analyses, as in earlier work [57], we instead emphasised the chemistry underlying the reactions. Amino-acid synthesis pathways were manually curated from the MetaCyc database [58] on the basis of their conservation between archaea and bacteria. Structuring metabolism around CO_2 fixation in this way generates a striking pattern. Amino acids encoded by G at the first position of the codon are clearly seen to be the first amino acids produced by the flux of carbon from the acetyl-CoA pathway into the reverse incomplete Krebs cycle. Amino acids encoded by A at the first base of the codon are predominantly the second set of amino acids produced from CO_2 and H_2, followed by C-encoded amino acids; U-encoded species are largely the furthest from CO_2 fixation.

This map makes an important distinction from the code coevolution hypothesis in its classical forms, which as noted earlier assume biosynthetic transformations occurring on peptidated tRNA molecules. Rather than the first codon position reflecting families of amino acids with similar biosynthetic relationships, our map points to a temporal patterning of amino acid recruitment into the genetic code. This has the potential to explain why some amino acids with distinct biosynthetic origins still have the same nucleotide at the first position in the codon, e.g. histidine and the glutamate derived amino acids. Initial weak CO_2 flux (in the context of growing protocells [51,52]) would mean that the highest concentration of amino acids would be those encoded by G at the first position. Note that we have limited the three hexacodonic amino acids (serine, arginine and leucine) to single first codon groups that best reflect their biosynthetic and temporal groups (A, C, C at the first codon, respectively). This is justified in the SI. To exclude bias in visual interpretation we have totalled the number of reaction steps from CO_2 for each amino acid. Fig. 2 shows that, while there is overlap between the species, there is a clear rise in the number of reaction steps required for the synthesis of each set of amino acids.

Given that each set of amino acids is associated with a specific first-position codon, we looked to see if a corresponding temporal ordering could be achieved for the cognate nucleotides. A direct relationship between the biosynthetic emergence of amino acids and nucleotides could explain why the earliest set of amino acids emerged at the same time as guanosine, for example, but we could not identify any temporal ordering with nucleotides. Guanosine and adenosine nucleotides are derived through the same number of steps, and just one step less than uridine. Worse, cytidine species are derived secondarily from uridine, so their recruitment of an earlier set of amino acids makes little sense.

In reality, the number of steps is a very loose guide to their likelihood. We are currently modelling the kinetic and thermodynamic probability of each step in the core pathways of metabolism, to determine the most likely patterns of flux. Glycine is the key amino acid for purine synthesis in the de novo pathway. The earliest synthesis pathway for glycine was probably direct assimilation from a methenyl-pterin species [59,60]. The CO_2 fixation pathway is rich in guanosine derived cofactors, notably methanopterins and folates, the C_1 carriers in methanogenesis and acetogenesis respectively, as well as flavins and molybdenum cofactors [59,61,62]. Together, these point to a positive feedback loop in which guanosine synthesis feeds back on CO_2 fixation and so glycine synthesis. Greater flux through any C_1H_2X species could increase glycine concentration, while in turn improving the yield of purine nucleotides.

Given that the temporal pattern predicts that purine-encoded amino acids were the earliest amino acids to be recruited to the genetic code (Fig. 1), combined with the identified positive feedback loop between guanosine cofactors, glycine, and purine synthesis, it seems possible that

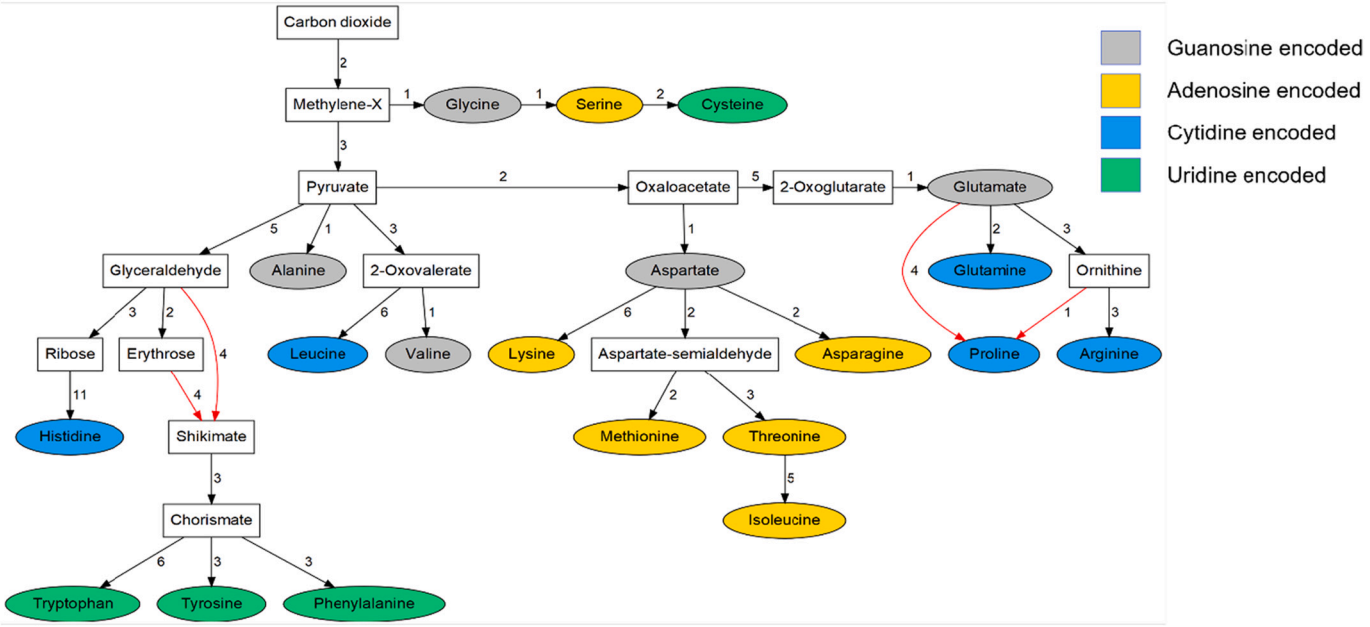

Fig. 1. Metabolic map showing reconstructed ancestral amino acid synthesis pathways.
Metabolism oriented around autotrophic CO_2 fixation via the acetyl-CoA pathway. Rectangular nodes represent branch point metabolites; oval-coloured nodes indicate amino acids. Edges (arrows) indicate reaction pathways between nodes. Black arrows indicate chemical mechanisms conserved between archaea and bacteria; red arrows indicate alternative pathways employed in each domain. Connections are labelled with the number of reaction steps between species; spontaneous reactions have been omitted. The amino acids are coloured according to the nucleotide at the first codon position (G in gray, A in yellow, C in blue and U in green). Pathway information was manually mined from the MetaCyc database [58]. Amino acids with multiple first codons are coloured in one of their respective nucleotides as discussed in the main text.

in the earliest stages of metabolic and code evolution there was an unequal purine to pyrimidine ratio (as others have postulated previously [5,12]). How the specific ordering of G – A – C – U came to exist remains unclear from a purely metabolic point of view. A possible explanation is that the nucleotides which form the strongest binding interactions (G and C both form three hydrogen bonds via classic Watson-Crick base paring) recruit before those with weaker interactions (A and U form two hydrogen bonds). If so, then these binding interactions could reflect early (chemical) selection for codon:anticodon interactions with strong binding interactions between small protometabolic equivalents of mRNA and tRNA.

3. The second codon position reflects amino acid hydrophobicity

Building on the assumption of a temporal phenomenon at the first position, we found a repeating pattern, in which the hydrophobicity of the amino acid encoded corresponds to the hydrophobicity of the base at the second position of the anticodon. This pattern further specifies codon assignments. We initially observed the pattern using the hydropathy scale of Kyte and Doolittle [63]. Specifically, the more hydrophilic the amino acid within the set of amino acids, the more likely it was to be associated with U. Conversely, the more hydrophobic the amino acid, the more likely it was to be associated with A. This broad association corresponds to earlier observations on stereochemical interactions within the code [1,10,19]. What is new here is that the pattern repeats across the four time periods corresponding to the bases at the first position of the codon (Fig. S1). This means that considering the timing of amino acid emergence with its hydrophobicity serves to specify two nucleotides in the codon-anticodon pair.

The repeating pattern is not perfect. In particular, the amino acids cysteine and arginine deviate from their expected trends. This may be addressed by considering that the Kyte-Doolittle hydropathy scale is based on the folding behaviour of modern proteins. Cysteine forms internal disulphide bridges and reactive thiols are often buried in the hydrophobic core of proteins to protect from oxidation [64]. Arginine's guanidinium group, remains charged across all pH ranges $\leq$10 [65] meaning that it is undoubtedly hydrophilic, yet its capacity to form cation-π interactions suggests some degree of hydrophobic interaction. Given these uncertainties relating to protein context, we investigated the validity of our hypothesis by considering a range of other hydrophobicity scales. Specifically, we compared the scales proposed by Hopp [66], Janin [67], LogP values determined by Tayar [68], Engleman [69] and Eisenberg [70]. Fig. S1 shows that the pattern, while still present, is obfuscated by a lack of uniform units of hydrophobicity, and variation in hydrophobicity assignments for some amino-acid species.

To mitigate these variations in hydrophobicity, we took inspiration from Trinquier and Sanejouand [71], who attempted to determine what effective property was best preserved in the genetic code. While we do not agree with all their reasoning, their determination of a mean hydrophobicity ranking from 43 discrete scales is an inspired choice. Fig. 3 shows violin plots based on these data. Three features stand out. First, when considering the mean values (red points) for each amino acid, the pattern of hydrophobic assignment for each 2′ nucleotide is consistent across all four first codon positions, with the only deviation being histidine (which we return to later). Second, the pattern of amino acid to nucleotide assignment is robust for the earliest two groups of amino acids, encoded by G and A at the first codon position (upper panels), but is less obvious for the later C and U groups (lower panels). Third, the hydrophobicity rankings exhibit substantial variation, confirming that hydrophobicity scales are highly variable, and so could easily misrepresent the actual biophysical interactions. Whether hydrophobicity itself or some related property such as partition energy [72] is reflected in the genetic code is therefore unclear; but it is nonetheless sufficient to explain some codon assignments. Regardless of whether hydrophobicity or partition energy provides the best measurement of the physicochemical properties of amino acids, we are specifically referring to direct interactions between amino acids and the second position of the anticodon, rather than to a later stage of enzyme catalysis as proposed by Caldararo and Di Giulio [71,72].

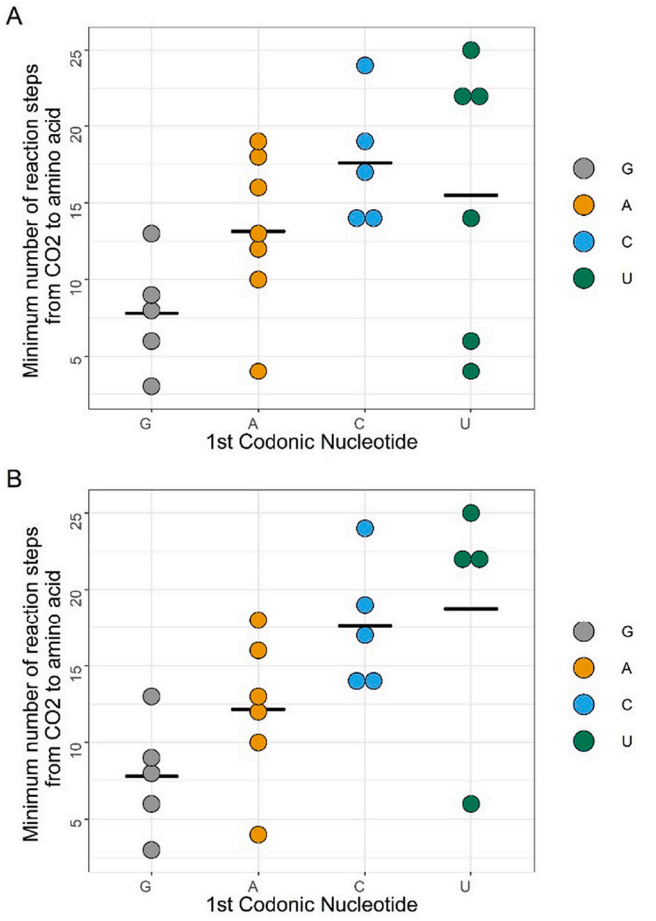

Fig. 2. Minimum number of reactions required for amino-acid synthesis from CO_2.
Amino acids are grouped by the nucleotide at the first position of the codon. The mean number of reaction steps is represented as a horizontal black bar. Panel A includes the dual assignment of the three hexacodonic nucleotides. Panel B shows these amino acids assigned to the single nucleotide group most consistent with their biosynthetic family and temporal ordering. The outlier amino acid with U at the first position of the codon is cysteine.

4. The third codon position corresponds to size in non-redundant codons

With our focus on the distinction between purines and pyrimidines, we noticed that the length of the amino acid can specify its allocation between non-redundant codons. Specifically, where sister codons NNR and NNY encode different amino acids (e.g. GAY = aspartate, GAR = glutamate) the identity of the nucleotide at the third position corresponds to the length of the amino acid encoded. Length in this context is the computed distance of the amino acid in its extended linear form [73] and does not consider alternative structural states. Fig. 4 shows this simple metric of amino acid length (maximal distance from carboxylic acid to the end of the R group) is consistent in six of these seven cases: the longer amino acid is assigned the NNR codon. This size dependency is direct for the codon (large amino acid, large purine base at the third position) but is inverted for the anticodon (large amino acid, small pyrimidine base at the third position of the codon). That implies an extension of the stereochemical effect at the third position of the anti-codon, which could specify the code assignment for an amino acid based on how well it fits into some unknown pocket.

Fascinatingly, this pattern appears to hold for the proteinogenic but non-standard amino acids. Pyrrolysine is encoded at the amber stop codon UAG. Tyrosine is encoded at the UAY codons. Pyrrolysine is longer than tyrosine, and in line with this pattern, should have a Y at the third position of the anti-codon. Selenocysteine is encoded by UGA, cysteine by UGY codons. While they have the same structure, the selenium atom is larger than the sulfur and this may be a sufficient difference to dictate a size-based discrimination. Further to this, these amino acids obey the expected rules of stereochemistry at the second position.

Examining this size-based relationship, we looked to see if there was any set of parameters in the structure of codons that could explain a binding pocket for amino acids. We failed to identify any patterns, but instead noticed that the position of redundant and non-redundant codons in the genetic code is not random. Fig. 5 shows an inverted code wheel, in which the third position is in the centre and the third position outermost. Clearly, redundancy is not randomly distributed around the genetic code and obeys specific rules which are entirely dependent on nucleotide sequence. This pattern allowed us to identify three rules which specify the locations of redundancy in the genetic code:

1. If there is a C in the second position of the codon (G in the second position of the anticodon) all codons **must** exhibit third position redundancy.
2. If there is an A in the second position of the codon (U in the second position of the anticodon) all codons **cannot** exhibit third position redundancy.
3. In instances where rules 1 or rule 2 do not apply (i.e. U or G in the second position of the codon), if there is a strong nucleotide (C or G) in the first codon position (S in the anticodon too) then all codons **must** exhibit third position redundancy.

Near identical rules have been reported before [74,75] in the context of translational optimisation, but our interpretation is subtly different as it links to both amino acid selection and code structure.

5. Predicting the full genetic code through temporal and stereochemical rules

If all 64 possible codons were to encode a separate species, there would be 64 different amino acids; as such, degeneracy is built into the code. The rules outlined above reduce the informational density of the genetic code to 24 units (Fig. 6A and B). Given that the standard code consists of 20 amino acids, three of which are hexacodonic (with two locations in the code, taking us up to a coding capacity of 23), and that there is a need to specify stop locations (getting up to 24), this reasoning constrains the 64 possible nucleotide permutations to the level that is observed throughout all life. This in turn suggests that the structure of the genetic code is in part determined by the nucleotide triplets themselves, perhaps due to conformational states they can form and how they interact with amino acids.

These codon sets can be used as template to assign specific amino acids. If we assume that the temporal pattern holds in its entirety, then following the order of G-A-C-U specified by the first position of the codon (Fig. 2), we can assign the four groups of amino acids to the quadrants shown in Fig. 6C, where the amino acids in each of the four groups are placed around the codon wheel. We assigned the hexacodonic amino acids (Ser, Arg and Leu) to the single codon group most in line with their biosynthetic origins. Next, we used the hydrophobic interactions at the second position of the anticodon to assign the amino acids in each quadrant, so that the most hydrophobic amino acid was assigned to the most hydrophobic nucleotide (A), and conversely, the most hydrophilic amino acid to most hydrophilic base (U) using the averaged hydrophobicity ranks from Fig. 3.

These assignments lead to a ‘first draft’ code, which nonetheless bears considerable similarity to the standard genetic code (Fig. 6D). The main issue here is that histidine (circled in red) is in the wrong place, as noted earlier for its hydrophobicity, which biases the assignments in the entire C codon quadrant. Correcting for the hydrophobicity of histidine is sufficient to correctly assign all C group amino acids (Fig. 6E). The

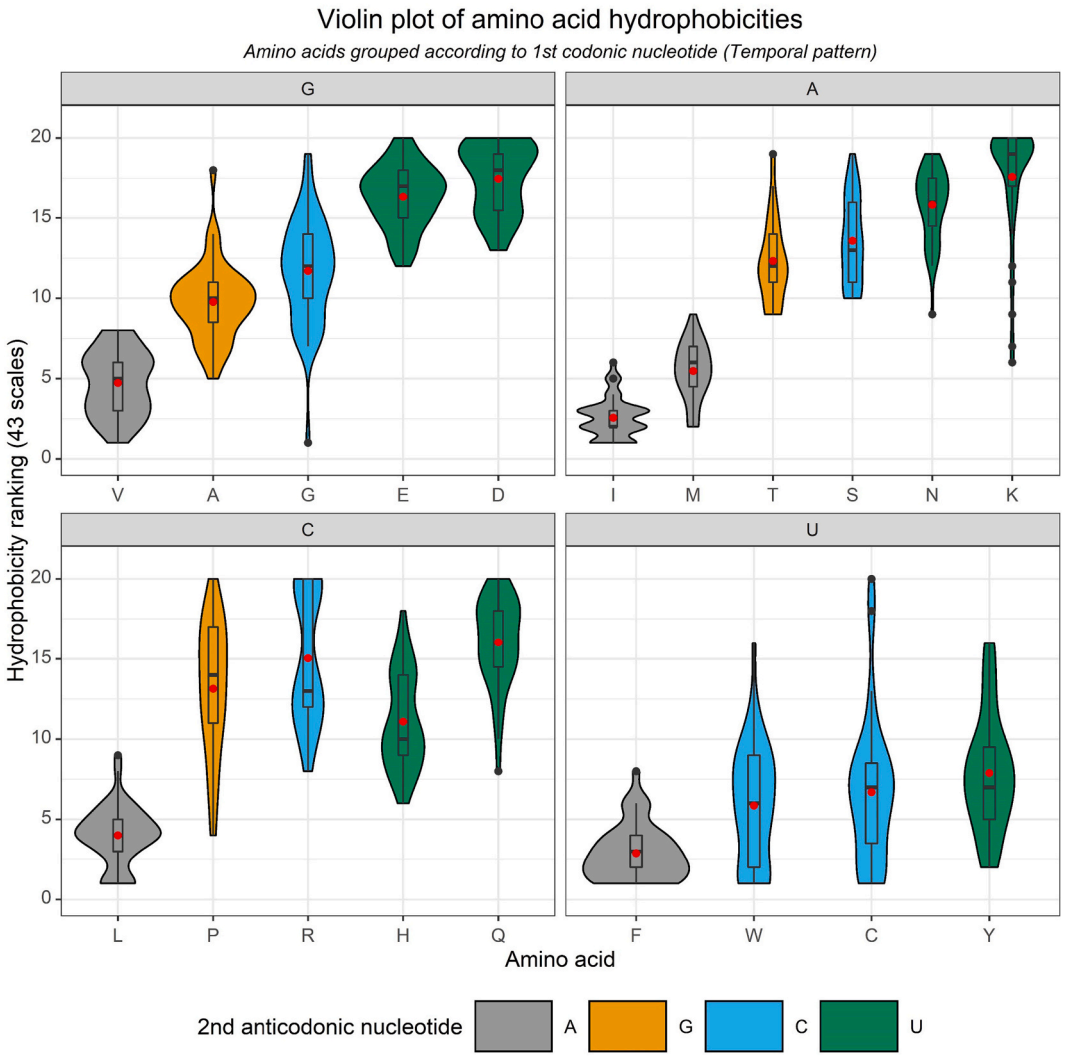

Fig. 3. Violin plots of amino acid mean and range hydrophobicity.
Amino acids are grouped according to the nucleotide at the first codon position, which we propose corresponds to a temporal grouping during the emergence of life. The violin plots are colour-coded according to the nucleotide at the second position of the anticodon, which is presumed to relate to stereochemical interactions. The hydrophobicity of the amino acid corresponds approximately to the hydrophobicity of the base at the second position. The red points show the mean ranking for each amino acid based on the method of Trinquier and Sanejouand [71] which ranks amino acids based on 43 separate scales of hydrophobicity. The boxplots show the median values (bold black bar) and the upper and lower quartiles, with the whiskers showing the upper or lower quartiles ± 1.5 * interquartile range.

reason that histidine specifically deviates is unknown. The question marks remaining in Fig. 6E are all in the U quadrant. These U-encoded amino acids are difficult to assign, as there are too many gaps in this section of the code.

Where there are two amino acids of similar hydrophobicity, which differ only at the third position, our assignments are based on size, with the longer amino acid assigned to NNR codons and the shorter one to NNY (Fig. 6E). Together, these assignments generate a code that has clear similarity to the extant genetic code. The remaining gaps distributed around the codon wheel are conveniently the codons utilised by the hexacodonic amino acids. The emergence of hexacodonic nucleotides could therefore be a simple space filling phenomenon (Fig. 6F), in which the amino acids filling these gaps are assigned to the code as appropriate, still following the stereochemical rules. Given that the AGR codons for arginine are commonly mutable in variant genetic codes [76] and that the reassignments are typically to stop codons or glycine or serine, both of which fulfil the same hydrophobicity position in alternative quadrants, this seems reasonable. There are a number of other factors not elucidated here that we discuss briefly in the SI, such as why methionine and tryptophan become single codon restricted, and why the biological non-coded amino acids generated in metabolism did not become incorporated into the genetic code. Applying these simple rules generates a codon table that is remarkably close to the standard genetic code. In fact, barring the assignment of AGR, our predicted code looks like several of the mitochondrial codes [77].

These observations are all drawn from patterns in the modern genetic code but are here interpreted through an autotrophic origins-of-life lens. Notwithstanding the remaining questions, our consideration of the code from an autotrophic point of view clearly makes sense of the emergence of translation from protometabolism. While we acknowledge some circularity in deriving the code from patterns found within the code, the simplest and arguably the only sensible interpretation of these patterns is that (i) they are real and strong enough to shine through billions of years of evolution; (ii) they reflect direct biophysical interactions between cognate amino acids and specific nucleotide sequences that developed over time as protometabolism itself expanded; and (iii) the precise interactions may not be between a naked anticodon and its amino acid but could be between short RNA aptamers with binding pockets and amino acids (as both codon and anticodon are involved in the patterns, and Watson-Crick base-pairing may play some role).

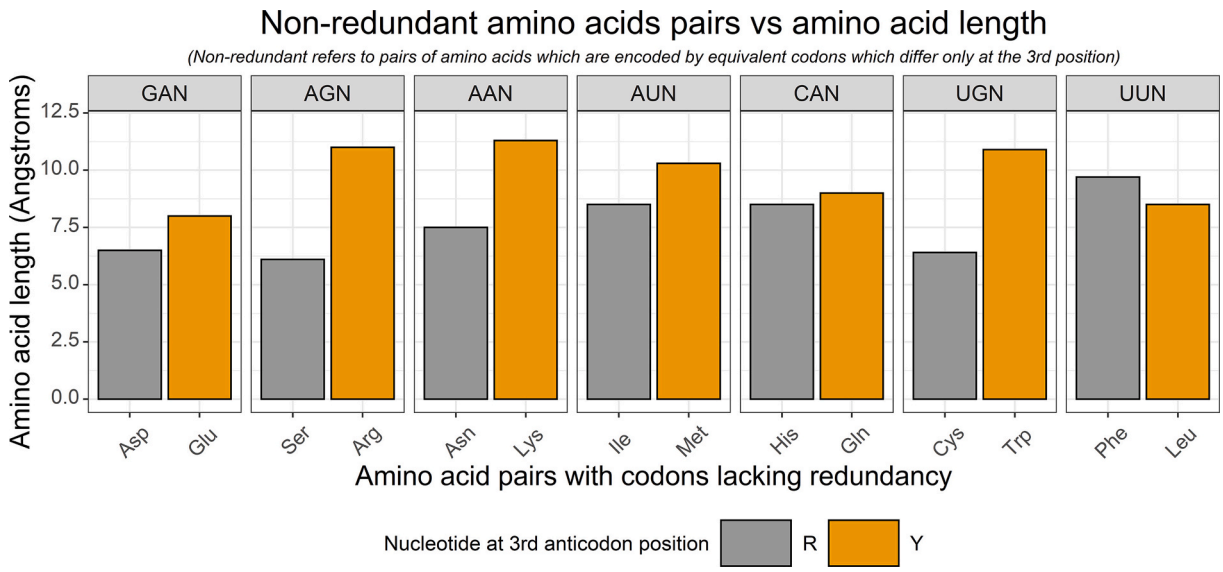

Fig. 4. Lengths of amino-acid pairs encoded by codons non-redundant at the third position.
Non-redundant pairs of amino acids have been grouped according to their codons and colour coded according to the nucleotide species present at their 3rd codon position. These pairs seem to show an overall trend that the smaller amino acid is associated with a smaller nucleotide at the third position of the codon, with pyrimidines (Y) being smaller than purines (R). Conversely, in the anticodon, the smaller amino acid is associated with the larger base, suggesting spatial constraints.

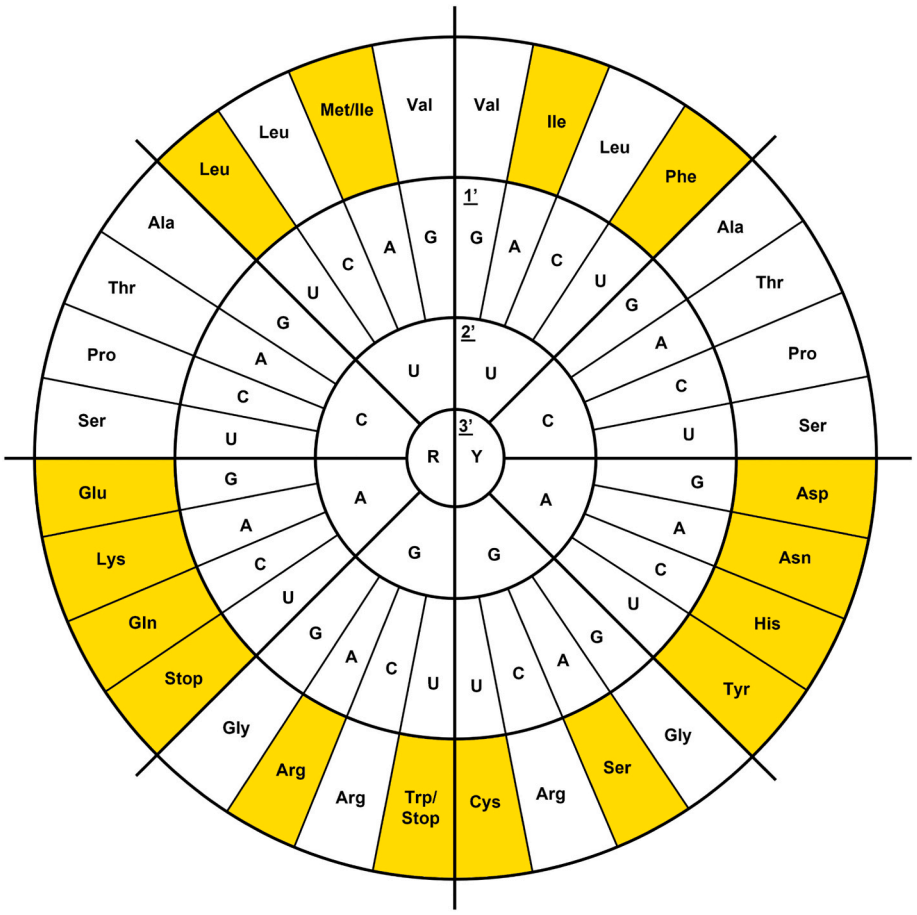

Fig. 5. Reversed codon table with redundant codons coloured.
The genetic code in wheel format, with the normal ring order for the codon sequence reversed. The innermost ring corresponds to the 3′ end of the codon, while the outermost ring corresponds to the 5′ end of the codon. The amino acids encoded by codon segments are labelled in the outermost ring. Non-redundant amino acids are coloured in yellow. The codon table, inverted in this way shows symmetry in the vertical axis; this is a product of the way the table is constructed. The pseudosymmetry which can be observed in the horizontal axis however indicates that redundancy in the genetic code is a non-random phenomenon that can be predicted by nucleotide sequence.

6. Conclusion

We have presented here a hypothesis on the origins of the genetic code, which is grounded in a reinterpretation of longstanding observations of patterns within the genetic code [1,2,19]. The rules we have identified effectively recapitulate the extant genetic code on the basis of spontaneous protometabolism from H_2 and CO_2 at the origin of life and some form of stereochemical interactions between nucleotides

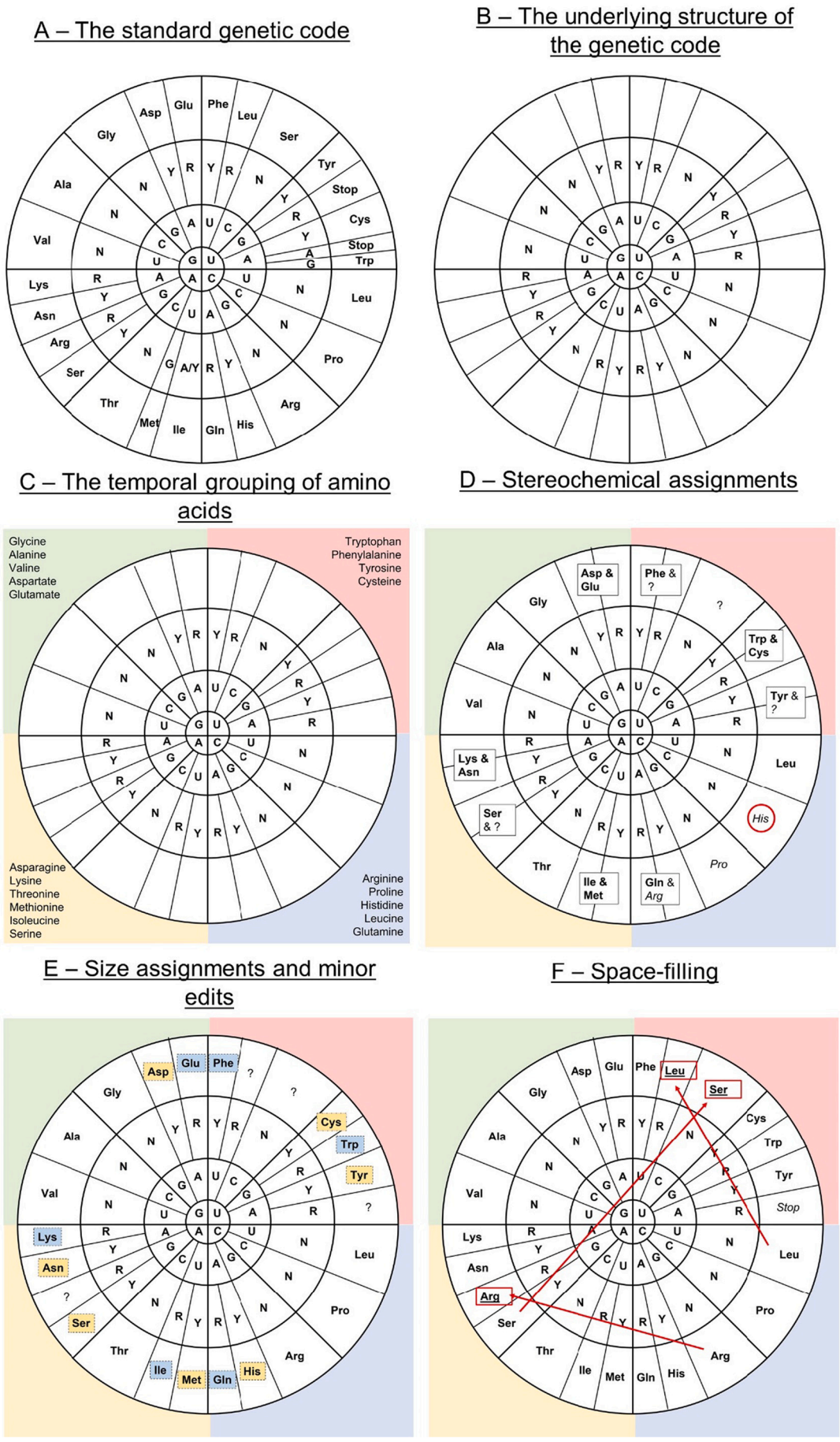

(caption on next page)

Fig. 6. Using identified rules to assign the genetic code.
(A) The standard genetic code, included for reference purposes. (B) The underlying structure of the genetic code obtained by following the rules of redundancy. (C) Temporal grouping of amino acids determined by mapping early metabolism from CO_2 fixation. (D) Stereochemical assignment for positions in each group (Most hydrophobic amino acid to most hydrophobic base and vice versa) using the averaged values in Fig. 3. Correct assignments in bold, incorrect assignments in italics. Histidine has been ringed in red as a major outlier which alters the assignment in the third temporal group. (E) Adding a further layer of assignment using the 3rd position size rules – longer amino acids (blue boxes) become associated with codons with a 3rd position R, smaller amino acids (yellow boxes) become associated with 3rd position Y, in instances where there is no competing amino acid the amino acid is also assigned 3rd position Y. In addition, we have corrected histidine's position. (F) Final space filling phenomenon to obtain a complete version of the genetic code.

and amino acids. We predict that these would involve direct non-covalent binding interactions between short aptamers of RNA and amino acids. Further work to confirm each rule in this specific context is underway, using NMR and molecular dynamic simulations. But the fact that longstanding patterns in the code are amplified and clarified by the assumption of strictly autotrophic protocellular origins lends credence to our interpretation.

Some complexities arise from the rules identified. In particular how could a temporal pattern on the *codon*, and a stereochemical pattern on the *anti-codon* co-emerge? The fact that these patterns are observed on both the codon and the anticodon may point to a three-component mechanism of early translation, as observed in life (i.e. codon, anti-codon, amino acid). Other important elements that are missing from this hypothesis concern the RNA species involved (proto-mRNA, proto-tRNA, proto-ribosome) which constitute the mechanistic components of the genetic code. We envision that only RNA species with the complexity of small interacting aptamers could ensure that amino acids are incorporated into the code in the temporal ordering observed or could underpin the weak stereochemical interactions that still shine through the code. While these specific interactions remain enigmatic, we note that they require no more than short polymers of RNA that lack any information content. Our scenario therefore offers a new perspective on the origins of information in biology. Any form of direct interactions, in which random RNA sequences interact in a non-random way with amino acids means that the sequence of amino acids in a nascent peptide would be templated by the RNA sequence. RNA aptamers with no intrinsic information content formed within growing protocells would be expected to have functions relating to protocell growth, such as CO_2 fixation, interactions with nucleotide cofactors, or copying the RNA sequences themselves (as the RNA polymerase is a Mg^{2+}-dependent protein, it is feasible that a short Mg^{2+}-binding peptide could partially mimic its function). The assumption of a spontaneous protometabolism in growing protocells therefore makes sense of the code within the codons, and simultaneously offers a framework that enables the transition from deterministic chemistry to genetic information at the origin of life.

Declaration of competing interest

The authors declare that they have no known competing financial interests or personal relationships that could have appeared to influence the work reported in this paper.

Data availability

Data will be made available on request.

Acknowledgements

This work was supported by funding from the Biotechnology and Biological Sciences Research Council to NL (BB/V003542/1) and from the Natural Environment Research Council to AH and NL (2236041).

Appendix A. Supplementary data

Supplementary data to this article can be found online at https://doi.org/10.1016/j.bbabio.2022.148597.

References

[1] F.J.R. Taylor, D. Coates, The code within the codons, Biosystems 22 (1989) 177–187, https://doi.org/10.1016/0303-2647(89)90059-2.
[2] J.T.-F. Wong, A co-evolution theory of the genetic code, Proc. Natl. Acad. Sci. 72 (1975) 1909–1912, https://doi.org/10.1073/pnas.72.5.1909.
[3] J.T.F. Wong, S.K. Ng, W.K. Mat, T. Hu, H. Xue, Coevolution theory of the genetic code at age forty: pathway to translation and synthetic life, Life 6 (2016) 12, https://doi.org/10.3390/LIFE6010012, 2016, Vol. 6, Page 12.
[4] C.R. Woese, The genetic code. the molecular basis for genetic expression. Carl R. Woese, Q. Rev. Biol. 43 (1968), https://doi.org/10.1086/405846, 327–327.
[5] L.E. Orgel, Evolution of the genetic apparatus, J. Mol. Biol. 38 (1968) 381–393, https://doi.org/10.1016/0022-2836(68)90393-8.
[6] A.D. Ellington, M. Khrapov, C.A. Shaw, The scene of a frozen accident, RNA 6 (2000) 485–498, https://doi.org/10.1017/S1355838200000224.
[7] M. Yarus, J.G. Caporaso, R. Knight, Origins of the genetic code: the escaped triplet theory, Annu. Rev. Biochem. 74 (2005) 179–198, https://doi.org/10.1146/annurev.biochem.74.082803.133119.
[8] M.A. Khaled, D.W. Mullins, M. Swindle, J.C. Lacey, Complexes of polyadenylic acid and the methyl esters of amino acids, Orig. Life 13 (1983) 87–96, https://doi.org/10.1007/BF00928886.
[9] J. Reuben, F.E. Polk, Nucleotide-amino acid interactions and their relation to the genetic code, J. Mol. Evol. 15 (1980) 103–112, https://doi.org/10.1007/BF01732664.
[10] M.K. Hobish, N.S.M.D. Wickramasinghe, C. Ponnamperuma, Direct interaction between amino acids and nucleotides as a possible physicochemical basis for the origin of the genetic code, Adv. Space Res. 15 (1995) 365–382, https://doi.org/10.1016/S0273-1177(99)80108-2.
[11] A.L. Weber, J.C. Lacey, Genetic code correlations: amino acids and their anticodon nucleotides, J. Mol. Evol 11 (3) (1978) 199–210, https://doi.org/10.1007/BF01734481.
[12] U. Baumann, J. Oro, Three stages in the evolution of the genetic code, Biosystems 29 (1993) 133–141, https://doi.org/10.1016/0303-2647(93)90089-U.
[13] J.C. Fontecilla-Camps, The stereochemical basis of the genetic code and the (mostly) autotrophic origin of life, Life 4 (2014) 1013–1025, https://doi.org/10.3390/LIFE4041013.
[14] Á. Kun, Á. Radványi, The evolution of the genetic code: impasses and challenges, Biosystems 164 (2018) 217–225, https://doi.org/10.1016/J.BIOSYSTEMS.2017.10.006.
[15] E.V. Koonin, A.S. Novozhilov, Origin and evolution of the genetic code: the universal enigma, IUBMB Life 61 (2009) 99, https://doi.org/10.1002/IUB.146.
[16] E.V. Koonin, Frozen accident pushing 50: stereochemistry, expansion, and chance in the evolution of the genetic code, Life 7 (2017) 22, https://doi.org/10.3390/LIFE7020022.
[17] M. Di Giulio, The coevolution theory of the origin of the genetic code, Phys Life Rev 1 (2004) 128–137, https://doi.org/10.1016/j.plrev.2004.05.001.
[18] M. di Giulio, An autotrophic origin for the coded amino acids is concordant with the coevolution theory of the genetic code, J. Mol. Evol. 83 (2016) 93–96, https://doi.org/10.1007/S00239-016-9760-X, 2016 83:3.
[19] S.D. Copley, E. Smith, H.J. Morowitz, A mechanism for the association of amino acids with their codons and the origin of the genetic code, Proc. Natl. Acad. Sci. 102 (2005) 4442–4447, https://doi.org/10.1073/pnas.0501049102.
[20] T. Yaman, J.N. Harvey, Computational Analysis of a Prebiotic Amino Acid Synthesis with Reference to Extant Codon-Amino Acid Relationships, 2021, https://doi.org/10.3390/life11121343.
[21] S.A. Harrison, N. Lane, Life as a guide to prebiotic nucleotide synthesis, Nat. Commun. 9 (2018) 5176, https://doi.org/10.1038/s41467-018-07220-y.
[22] G. Fuchs, Alternative pathways of carbon dioxide fixation: insights into the early evolution of Life? Annu. Rev. Microbiol. 65 (2011) 631–658, https://doi.org/10.1146/annurev-micro-090110-102801.
[23] N. Lane, J.F. Allen, W. Martin, How did LUCA make a living? Chemiosmosis in the origin of life, BioEssays 32 (2010) 271–280, https://doi.org/10.1002/bies.200900131.
[24] S.D. Copley, E. Smith, H.J. Morowitz, The origin of the RNA world: co-evolution of genes and metabolism, Bioorg. Chem. 35 (2007) 430–443, https://doi.org/10.1016/J.BIOORG.2007.08.001.
[25] M.J. Russell, A.J. Hall, The emergence of life from iron monosulphide bubbles at a submarine hydrothermal redox and pH front, J. Geol. Soc. Lond. 154 (1997) 377–402, https://doi.org/10.1144/gsjgs.154.3.0377.
[26] G. Wächtershäuser, Evolution of the first metabolic cycles, Proc. Natl. Acad. Sci. 87 (1990) 200–204, https://doi.org/10.1073/pnas.87.1.200.
[27] E. Smith, H.J. Morowitz, Universality in intermediary metabolism, Proc. Natl. Acad. Sci. U. S. A. 101 (2004) 13168–13173, https://doi.org/10.1073/pnas.0404922101.

[28] M.J. Russell, W. Martin, The rocky roots of the acetyl-CoA pathway, Trends Biochem. Sci. 29 (2004) 358–363, https://doi.org/10.1016/J.TIBS.2004.05.007.
[29] W. Martin, M.J. Russell, On the origin of biochemistry at an alkaline hydrothermal vent, Philos. Trans. R. Soc., B 362 (2007) 1887–1926, https://doi.org/10.1098/rstb.2006.1881.
[30] J.P. Amend, T.M. McCollom, in: Energetics of Biomolecule Synthesis on Early Earth, 2010, pp. 63–94, https://doi.org/10.1021/bk-2009-1025.ch004.
[31] J.P. Amend, D.E. LaRowe, T.M. McCollom, E.L. Shock, The energetics of organic synthesis inside and outside the cell, Philos. Trans. R. Soc. Lond. Ser. B Biol. Sci. 368 (2013), 20120255, https://doi.org/10.1098/rstb.2012.0255.
[32] E.L. Shock, M.D. Schulte, Organic synthesis during fluid mixing in hydrothermal systems, J. Geophys. Res. Planets 103 (1998) 28513–28527, https://doi.org/10.1029/98JE02142.
[33] J.P. Amend, E.L. Shock, Energetics of overall metabolic reactions of thermophilic and hyperthermophilic archaea and bacteria, FEMS Microbiol. Rev. 25 (2001) 175–243, https://doi.org/10.1111/j.1574-6976.2001.tb00576.x.
[34] M. Preiner, K. Igarashi, K.B. Muchowska, M. Yu, S.J. Varma, K. Kleinermanns, M. K. Nobu, Y. Kamagata, H. Tüysüz, J. Moran, W.F. Martin, A hydrogen-dependent geochemical analogue of primordial carbon and energy metabolism, Nat. Ecol. Evol. 4 (2020) 534–542, https://doi.org/10.1038/s41559-020-1125-6.
[35] S.J. Varma, K.B. Muchowska, P. Chatelain, J. Moran, Native iron reduces CO2 to intermediates and end-products of the acetyl-CoA pathway, Nat. Ecol. Evol. (2018) 1, https://doi.org/10.1038/s41559-018-0542-2.
[36] K.B. Muchowska, S.J. Varma, E. Chevallot-Beroux, L. Lethuillier-Karl, G. Li, J. Moran, Metals promote sequences of the reverse Krebs cycle, Nat. Ecol. Evol. 1 (2017) 1716–1721, https://doi.org/10.1038/s41559-017-0311-7.
[37] M.A. Keller, A.V. Turchyn, M. Ralser, Non-enzymatic glycolysis and pentose phosphate pathway-like reactions in a plausible Archean Ocean, Mol. Syst. Biol. 10 (2014) 725, https://doi.org/10.1002/MSB.20145228.
[38] G. Piedrafita, S.J. Varma, C. Castro, C.B. Messner, L. Szyrwiel, J.L. Griffin, M. Ralser, Cysteine and iron accelerate the formation of ribose-5-phosphate, providing insights into the evolutionary origins of the metabolic network structure, PLoS Biol. 19 (2021), https://doi.org/10.1371/JOURNAL.PBIO.3001468.
[39] C.B. Messner, P.C. Driscoll, G. Piedrafita, M.F.L. De Volder, M. Ralser, Nonenzymatic gluconeogenesis-like formation of fructose 1,6-bisphosphate in ice, Proc. Natl. Acad. Sci. 114 (2017) 7403–7407, https://doi.org/10.1073/pnas.1702274114.
[40] C. Huber, G. Wächtershäuser, Primordial reductive amination revisited, Tetrahedron Lett. 44 (2003) 1695–1697, https://doi.org/10.1016/S0040-4039(02)02863-0.
[41] L.M. Barge, E. Flores, M.M. Baum, D.G. VanderVelde, M.J. Russell, Redox and pH gradients drive amino acid synthesis in iron oxyhydroxide mineral systems, Proc. Natl. Acad. Sci. 116 (2019) 4828–4833, https://doi.org/10.1073/pnas.1812098116.
[42] R.J. Mayer, H. Kaur, S.A. Rauscher, J. Moran, Mechanistic insight into metal ion-catalyzed transamination, J. Am. Chem. Soc. 143 (2021) 42, https://doi.org/10.1021/jacs.1c08535.
[43] T.M. Mccollom, G. Ritter, B.R.T. Simoneit, Lipid synthesis under hydrothermal conditions by fischer-tropsch-type reactions, Orig. Life Evol. Biosph. 29 (1999) 153–166, https://doi.org/10.1023/A:1006592502746.
[44] D. He, X. Wang, Y. Yang, R. He, H. Zhong, Y. Wang, B. Han, F. Jin, Hydrothermal synthesis of long-chain hydrocarbons up to C 24 with NaHCO 3 -assisted stabilizing cobalt, Proc. Natl. Acad. Sci. 118 (2021), https://doi.org/10.1073/pnas.2115059118.
[45] M.J. Russell, Cobalt: a must-have element for life and livelihood, Proc. Natl. Acad. Sci. U. S. A. 119 (2022), https://doi.org/10.1073/PNAS.2121307119.
[46] J. Yi, H. Kaur, W. Kazöne, S.A. Rauscher, L.-A. Gravillier, K.B. Muchowska, J. Moran, A nonenzymatic analog of pyrimidine nucleobase biosynthesis, Angew. Chem. Int. Ed. (2022), e202117211, https://doi.org/10.1002/ANIE.202117211.
[47] R. Hudson, R. de Graaf, M. Strandoo Rodin, A. Ohno, N. Lane, S.E. McGlynn, Y.M. A. Yamada, R. Nakamura, L.M. Barge, D. Braun, V. Sojo, CO_2 reduction driven by a pH gradient, Proc. Natl. Acad. Sci. 117 (2020) 22873–22879, https://doi.org/10.1073/pnas.2002659117.
[48] V. Sojo, B. Herschy, A. Whicher, E. Camprubi, N. Lane, The origin of life in alkaline hydrothermal vents, Astrobiology 16 (2) (2016) 181–197, https://doi.org/10.1089/ast.2015.1406.
[49] N. Lane, W.F. Martin, The origin of membrane bioenergetics, Cell 151 (2012) 1406–1416, https://doi.org/10.1016/J.CELL.2012.11.050.
[50] R. Vasiliadou, N. Dimov, N. Szita, S.F. Jordan, N. Lane, Possible mechanisms of CO2 reduction by H2 via prebiotic vectorial electrochemistry, Interface Focus 9 (2019), https://doi.org/10.1098/RSFS.2019.0073.
[51] T. West, V. Sojo, A. Pomiankowski, N. Lane, The origin of heredity in protocells, Philos. Trans. R. Soc., B 372 (2017), https://doi.org/10.1098/RSTB.2016.0419.
[52] R.N. Palmeira, M. Colnaghi, S.A. Harrison, A. Pomiankowski, N. Lane, The Limits of Metabolic Heredity in Protocells, BioRxiv, 2022, https://doi.org/10.1101/2022.01.28.477904.
[53] S.F. Jordan, H. Rammu, I.N. Zheludev, A.M. Hartley, A. Maréchal, N. Lane, Promotion of protocell self-assembly from mixed amphiphiles at the origin of life, Nat. Ecol. Evol. (2019), https://doi.org/10.1038/s41559-019-1015-y.
[54] S.F. Jordan, E. Nee, N. Lane, Isoprenoids Enhance the Stability of Fatty Acid Membranes at the Emergence of Life Potentially Leading to an Early Lipid Divide, 2019, https://doi.org/10.1098/rsfs.2019.0067.
[55] S.F. Jordan, I. Ioannou, H. Rammu, A. Halpern, L.K. Bogart, M. Ahn, R. Vasiliadou, J. Christodoulou, A. Maréchal, N. Lane, Spontaneous assembly of redox-active iron-sulfur clusters at low concentrations of cysteine, Nat. Commun. 12 (2021) 1–14, https://doi.org/10.1038/s41467-021-26158-2, 2021 12:1.
[56] T.L. Hendrickson, W.N. Wood, U.M. Rathnayake, Did Amino Acid Side Chain Reactivity Dictate the Composition and Timing of Aminoacyl-tRNA Synthetase Evolution?, 2021, https://doi.org/10.3390/genes.
[57] M.C. Weiss, F.L. Sousa, N. Mrnjavac, S. Neukirchen, M. Roettger, S. Nelson-Sathi, W.F. Martin, The physiology and habitat of the last universal common ancestor, Nat. Microbiol. 1 (2016) 16116, https://doi.org/10.1038/nmicrobiol.2016.116.
[58] R. Caspi, R. Billington, I.M. Keseler, A. Kothari, M. Krummenacker, P.E. Midford, W.K. Ong, S. Paley, P. Subhraveti, P.D. Karp, The MetaCyc database of metabolic pathways and enzymes - a 2019 update, Nucleic Acids Res. 48 (2020), https://doi.org/10.1093/NAR/GKZ862. D455–D453.
[59] R. Braakman, E. Smith, The emergence and early evolution of biological carbon-fixation, PLoS Comput. Biol. 8 (2012), e1002455, https://doi.org/10.1371/journal.pcbi.1002455.
[60] G.Ceren Tok, A.Teresa Sophie Freiberg, L. Reinschlüssel, I. Emahi, P.R. Gruenke, R. Braakman, E. Smith, The compositional and evolutionary logic of metabolism, Phys. Biol. 10 (2012), 011001, https://doi.org/10.1088/1478-3975/10/1/011001.
[61] B.E.H. Maden, Tetrahydrofolate and tetrahydromethanopterin compared: functionally distinct carriers in C1 metabolism, Biochem. J. 350 (2000) 609–629, https://doi.org/10.1042/bj3500609.
[62] H.B. White, Coenzymes as fossils of an earlier metabolic state, J. Mol. Evol. 7 (2) (1976) 101–104, https://doi.org/10.1007/BF01732468.
[63] J. Kyte, R.F. Doolittle, A simple method for displaying the hydropathic character of a protein, J. Mol. Biol. 157 (1982) 105–132, https://doi.org/10.1016/0022-2836(82)90515-0.
[64] J.J.A.G. Kamps, R.J. Hopkinson, C.J. Schofield, T.D.W. Claridge, How formaldehyde reacts with amino acids, Commun. Chem. 2 (2019) 1–14, https://doi.org/10.1038/s42004-019-0224-2, 2019 2:1.
[65] M.J. Harms, J.L. Schlessman, G.R. Sue, E.B. García-Moreno, Arginine residues at internal positions in a protein are always charged, Proc. Natl. Acad. Sci. 108 (2011) 18954–18959, https://doi.org/10.1073/pnas.1104808108.
[66] T.P. Hopp, K.R. Woods, A computer program for predicting protein antigenic determinants, Mol. Immunol. 20 (1983) 483–489, https://doi.org/10.1016/0161-5890(83)90029-9.
[67] J. Janin, Surface and inside volumes in globular proteins, Nature 277 (1979) 491–492, https://doi.org/10.1038/277491a0.
[68] N. El Tayar, R.-S. Tsai, P.-A. Carrupt, B. Testa, Octan-I-01-Water Partition Coefficients of Zwitterionic a-Amino Acids. Determination by Centrifugal Partition Chromatography and Factorization into Steric/Hydrophobic and Polar Components, 1992, https://doi.org/10.1039/P29920000079.
[69] D.M. Engelman, T.A. Steitz, A. Goldman, Identifiying nonpolar transbilayer helicines in amino acid seuqneces of membrane proteins, Annu. Rev. Biophys. Biophys. Chem. 15 (1986) 321–353, https://doi.org/10.1146/annurev.bb.15.060186.001541.
[70] D. Eisenberg, E. Schwarz, M. Komaromy, R. Wall, Analysis of membrane and surface protein sequences with the hydrophobic moment plot, J. Mol. Biol. 179 (1984) 125–142, https://doi.org/10.1016/0022-2836(84)90309-7.
[71] G. Trinquier, Y.H. Sanejouand, Which effective property of amino acids is best preserved by the genetic code? Protein Eng. Des. Sel. 11 (1998) 153–169, https://doi.org/10.1093/protein/11.3.153.
[72] F. Caldararo, M. di Giulio, The genetic code is very close to a global optimum in a model of its origin taking into account both the partition energy of amino acids and their biosynthetic relationships, Biosystems 214 (2022), 104613, https://doi.org/10.1016/j.biosystems.2022.104613.
[73] C.B. Ching, K. Hidajat, M.S. Uddin, Evaluation of equilibrium and kinetic parameters of smaller molecular size amino acids on KX zeolite crystals via liquid chromatographic techniques, Sep. Sci. Technol. 24 (1989) 581–597, https://doi.org/10.1080/01496398908049793.
[74] U. Lagerkvist, "Two out of three": an alternative method for codon reading, Proc. Natl. Acad. Sci. 75 (1978) 1759–1762, https://doi.org/10.1073/pnas.75.4.1759.
[75] U. Lagerkvist, Unorthodox codon reading and the evolution of the genetic code, Cell 23 (1981) 305–306, https://doi.org/10.1016/0092-8674(81)90124-0.
[76] R.D. Knight, S.J. Freeland, L.F. Landweber, Rewiring the keyboard: evolvability of the genetic code, Nat. Rev. Genet. 2 (2001) 49–58, https://doi.org/10.1038/35047500, 2001 2:1.
[77] A. Elzanowski, J. Ostell, The genetic codes,National Centre for Biotechnology Information. https://www.ncbi.nlm.nih.gov/Taxonomy/taxonomyhome.html/index.cgi?chapter=cgencodes, 2019.